CSIRO PUBLISHING

www.publish.csiro.au/journals/pasa *Publications of the Astronomical Society of Australia*, 2009, **26**, 209–216

Time-Scales of the *s* Process: from Minutes to Ages

F. Käppeler[A,G], *S. Bisterzo*[B], *R. Gallino*[B], *M. Heil*[C], *M. Pignatari*[D,E], *R. Reifarth*[C], *O. Straniero*[F], *S. Walter*[A], *N. Winckler*[C], *and K. Wisshak*[A]

[A] Forschungszentrum Karlsruhe, Institut für Kernphysik, P.O. Box 3640, D-76021 Karlsruhe, Germany
[B] Dipartimento di Fisica Generale, Università di Torino, Via P. Giuria 1, I-10125 Torino, Italy
[C] GSI Darmstadt, Planckstr. 1, D-64291 Darmstadt, Germany
[D] Keele University, Keele, Staffordshire ST5 5BG, UK
[E] Joint Institute for Nuclear Astrophysics, University of Notre Dame, Notre Dame, IN 46556, USA
[F] Osservatorio Astronomico di Collurania, I-64100 Teramo, Italy
[G] Corresponding author. Email: franz.kaeppeler@ik.fzk.de

Received 2008 November 21, accepted 2008 December 22

Abstract: The time scales in the *s* process appears to be an approriate aspect to discuss at the occasion of Roberto's 70th anniversary, the more as this subject has been repeatedly addressed during the 20 years of collaboration between Torino and Karlsruhe. The two chronometers presented in this text were selected to illustrate the intense mutual stimulation of both groups. Based on a reliable set of accurate stellar (n, γ) cross sections determined mostly at FZK, the Torino group succeeded to develop a comprehensive picture of the various *s*-process scenarios, which are most valuable for understanding the composition of the solar system as well as for the interpretation of an increasing number of astronomical observations.

Keywords: stars: AGB — nuclear reactions, nucleosynthesis, abundances — time

1 Introduction

The question of time scales is directly related to a number of key issues in *s*-process nucleosynthesis and from the very beginning the corresponding chronometers were considered to represent an important source of information. The long-lived radioactivities, which are produced in the *s* process, were studied first because of their cosmological importance and since they are less sensitive to details of stellar scenarios. But in principle any unstable isotope along the *s*-process reaction path can be understood as a potential chronometer, provided that it defines a time scale corresponding to a significant quantity.

The shortest possible time scale is related to *convective mixing in He shell flashes*, which take place in thermally pulsing low mass Asymptotic Giant Branch (AGB) stars, where turnover times of the less than an hour are attained (Section 2).

Neutron capture occurs on time scales of days to years, depending on the *s*-process scenario. The life time of a given isotope A is determined by the stellar-neutron flux, $n_n \times v_T$, and by the stellar (n, γ) cross section:

$$\tau_n(A) = \frac{1}{\lambda_n(A)} = \frac{1}{n_n \times v_T \times \sigma(A)}, \qquad (1)$$

where n_n denotes the neutron density and v_T the mean thermal velocity. If isotope A is unstable against β-decay with a life time comparable to λ_n, the reaction path is split into a branching with a characteristic abundance pattern that reflects this time scale and provides a measure for the neutron density at the stellar site (Best et al. 2001; Wisshak et al. 2001). This situation can be complicated by the fact that in most cases only theoretical evaluations are available for the neutron capture cross sections of the unstable isotopes. Furthermore, the β-decay rate of the branch point isotope A may depend on temperature and/or electron density of the stellar plasma as in case of ^{176}Lu (Section 3).

If the neutron capture time is comparable to the *duration of the neutron bursts*, the abundance pattern of such a branching can be used to test the time scale of the He shell flashes in AGB stars. Suited branchings of this type could be those at ^{85}Kr and ^{95}Zr with neutron capture times of a few years. In these cases, the neutron flux dies out before reaction equilibrium is achieved. However, both branchings are difficult to analyze because of significant contributions from the weak *s*-process component from massive stars or from the *r* process, and a constraining analysis is difficult to achieve.

The *transport to the stellar surface* in the third dredge-up phase can be investigated by means of the observed Tc abundances (Mathews et al. 1986; Smith & Lambert 1988; Busso et al. 1995). Analyses of these observations have to consider that the terrestrial decay rate of ^{99}Tc ($t_{1/2} = 2.1 \times 10^5$ years) is reduced to a few years at *s*-process temperatures (Schatz 1983; Takahashi & Yokoi 1987), which implies that it is quickly cooled to temperatures below 10^8 K after its production. A complementary, temperature-independent chronometer for the

© Astronomical Society of Australia 2009 10.1071/AS08052 1323-3580/09/03209

Downloaded from https://www.cambridge.org/core. IP address: 3.89.132.163, on 17 Jan 2022 at 00:26:57, subject to the Cambridge Core terms of use, available at https://www.cambridge.org/core/terms. https://doi.org/10.1071/AS08052

third dredge-up is ^{93}Zr, which can be followed by the appearance of its daughter ^{93}Nb (Mathews et al. 1986).

The time scale for the *formation of the solar system* can, in principle, be inferred from the abundance patterns, which are affected by the decay of nuclei with half-lives between 10^5 and 10^7 years (Pagel 1990). Quantitative studies based on isotopic anomalies found in presolar grains have confirmed that such effects exist for ^{26}Al, ^{41}Ca, ^{60}Fe, ^{93}Zr, and ^{107}Pd. A comprehensive overview of this discussion was presented by Busso, Gallino & Wasserburg (1999) (see also the contribution by R. Reifarth to this volume). Also ^{205}Pb was discussed as a potentially promising chronometer (Yokoi, Takahashi & Arnould 1985), whereas ^{53}Mn, ^{129}I, and ^{182}Hf were found to result from the continuous pollution of the interstellar medium by explosive nucleosynthesis in supernovae (Busso, Gallino & Wasserburg 1999).

A number of attempts have been made to constrain the *cosmic time scale* by means of *s*-process abundance information. In the course of these studies it turned out that the half-life of the most promising case, ^{176}Lu (Audouze, Fowler & Schramm 1972; Arnould 1973), was strongly temperature-dependent, making it an *s*-process thermometer rather than a cosmic clock as discussed in Section 3. The other long-lived species, ^{40}K (Beer & Penzhorn 1987) and ^{87}Rb (Beer & Walter 1984) are produced by at least two different processes and are difficult to interpret quantitatively. Therefore, recent analyses of nuclear chronometers for constraining the cosmic time scale concentrate on the *r*-process clocks related to the decay of the long-lived actinides (Cowan et al. 1999) and of ^{187}Re (Yokoi, Takahashi & Arnould 1983; Arnould, Takahashi & Yokoi 1984; Mosconi et al. 2007; see also the contribution by A. Mengoni to this volume).

In the following sections we will focus on the shortest *s*-process time scale related to the fast convective mixing during the He shell flashes in AGB stars.

2 The Branching at ^{128}I

Xenon is an element of considerable astrophysical interest. The origin of the lightest isotopes, ^{124}Xe and ^{126}Xe, can be exclusively ascribed to the so-called *p* process in supernovae (Arnould & Goriely 2003). Their relative isotopic abundances are important for testing *p*-process models describing the proton-rich side of the valley of stability. Concerning the *s* process, xenon belongs to the six elements with a pair of *s*-only isotopes. In this case, the relevant nuclei are ^{128}Xe and ^{130}Xe, both shielded against the decay chains from the *r*-process region by their stable Te isobars. The abundances of these isotopes define the strength of the branching in the *s*-process reaction chain illustrated in Figure 1. Since the *p*-process components of these *r*-shielded nuclei do not exceed a few percent, they are commonly considered to be of pure *s* origin. On the neutron-rich side, ^{134}Xe and ^{136}Xe can be ascribed to the *r* process since the β^- half life of ^{133}Xe is short enough to prevent any significant *s*-process contributions. Hence, the Xe isotope chain carries signatures of all nucleosynthesis

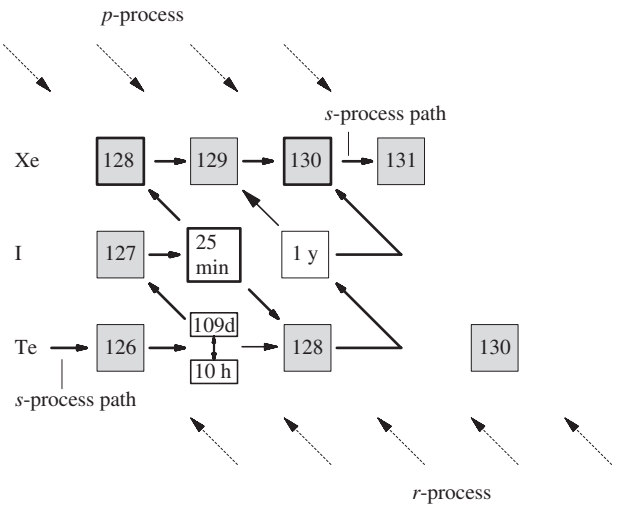

Figure 1 The *s*-process reaction path between Te and Xe. The isotopes ^{128}Xe and ^{130}Xe are shielded against *r*-process contributions by their stable Te isobars. In contrast to ^{130}Xe, ^{128}Xe is partly bypassed due to the branching at ^{128}I. The branching at ^{127}Te is negligible unless the temperature is low enough that ground state and isomer are not fully thermalized. The branching at ^{128}I is unique since it results from the competition between β^- and electron capture decays and is, therefore, independent of the neutron flux.

scenarios that contribute to the mass region of the heavy isotopes with $A \geq 90$, and offers the possibility to constrain the underlying models. A detailed description of the isotopic abundance pattern of xenon involves necessarily quantitative models for all these processes.

The combined strength of the branchings in the *s*-process chain at ^{127}Te and ^{128}I (Figure 1) is defined by the relative abundances of the *s*-only isotopes ^{128}Xe and ^{130}Xe. Both branchings are expected to be comparably weak since only a small part of the total reaction flow is bypassing ^{128}Xe. Therefore, the $\langle\sigma\rangle N_s$ value for ^{128}Xe, which is characteristic of the reaction flow, is slightly smaller than the one for ^{130}Xe. Since the solar isotopic ratio of the *s*-only isotopes is well defined (Pepin, Becker & Rider 1995), the $\langle\sigma\rangle N_s$ difference can be obtained by an accurate measurement of the cross section ratio (Reifarth et al. 2002).

While the first branching at ^{127}Te is marginal because the population of ground state and isomer is quickly thermalized in the hot stellar photon bath (Takahashi & Yokoi 1987), leading to a strong dominance of the β-decay channel, the second branching at ^{128}I is utterly interesting. In contrast to all other relevant cases, this branching is only defined by the competition between β^- and electron capture decay (Figure 1). Both decay modes are sufficiently short-lived that the neutron capture channel and hence the influence of the stellar-neutron flux is completely negligible.

Since the electron capture rate is sensitive to temperature and electron density of the stellar plasma Takahashi & Yokoi (1987), this branching provides a unique possibility to constrain these parameters without interference from the neutron flux. Under stellar

Downloaded from https://www.cambridge.org/core. IP address: 3.89.132.163, on 17 Jan 2022 at 00:26:57, subject to the Cambridge Core terms of use, available at https://www.cambridge.org/core/terms. https://doi.org/10.1071/AS08052

Table 1. β-Decay branching ratio

n_e (10^{26} cm^{-3})	Temperature (10^8 K)			
	0	1	2	3
0	0.940	0.963	0.996	0.999
3	0.940	0.952	0.991	0.997
10	0.940	0.944	0.976	0.992
30	0.940	0.938	0.956	0.980

conditions the corresponding branching ratio at ^{128}I is

$$f_- = \lambda_{\beta^-}/(\lambda_{\beta^-} + \lambda_{\beta^{EC}}) = 1 - \lambda_{\beta^{EC}}/(\lambda_{\beta^-} + \lambda_{\beta^{EC}}).$$

While the β^--rate varies only weakly, the electron capture rate depends strongly on temperature due to the increasing degree of ionization. Furthermore, at high temperatures, when the ions are fully stripped, the EC rate becomes sensitive to the density in the stellar plasma via electron capture from the continuum (Table 1). The relatively small change of the branching ratio did not permit quantitative analyses until the stellar (n, γ) rates of the involved isotopes were measured to an accuracy of 1.5% (Reifarth et al. 2002).

2.1 Thermally Pulsing AGB Stars

The *s*-process abundances in the mass range $A \geq 90$ are produced during helium shell burning in thermally pulsing low mass AGB stars (Straniero et al. 1995) by the subsequent operation of two neutron sources. The ^{13}C$(\alpha, n)^{16}$O reaction, which occurs under radiative conditions at low temperatures ($kT \approx 8$ keV) and neutron densities ($n_n \leq 10^7$ cm^{-3}) between convective He-shell burning episodes, provides most of the neutron exposure. The resulting abundances are modified by a second burst of neutrons from the ^{22}Ne$(\alpha, n)^{25}$Mg reaction, which is marginally activated during the highly convective He shell flashes, when peak neutron densities of $n_n \geq 10^{10}$ cm^{-3} are reached at $kT \approx 23$ keV. Although this second neutron burst accounts only for a few percent of the total neutron exposure, it is essential for adjusting the final abundance patterns of the *s*-process branchings. It is important to note that the (n, γ) cross sections in the Te–I–Xe region are large enough that typical neutron capture times are significantly shorter than the duration of the two neutron exposures. Therefore, the abundances can follow the time variations of the neutron density.

2.2 Convection in He Shell Flashes

The effect of convection for the branchings at $A = 127/128$ was extensively studied by means of the stellar evolution code FRANEC (Chieffi & Straniero 1989; Straniero et al. 1997) using a time-dependent mixing algorithm to treat the short time scales during thermal pulses along the AGB. Convective velocities were evaluated by means of the mixing length theory where the mixing length parameter was calibrated by a fit of the solar radius. An example for these results is given in Figure 2, which represents a typical thermal pulse for a 3-$M_\odot$ AGB star of solar composition. The

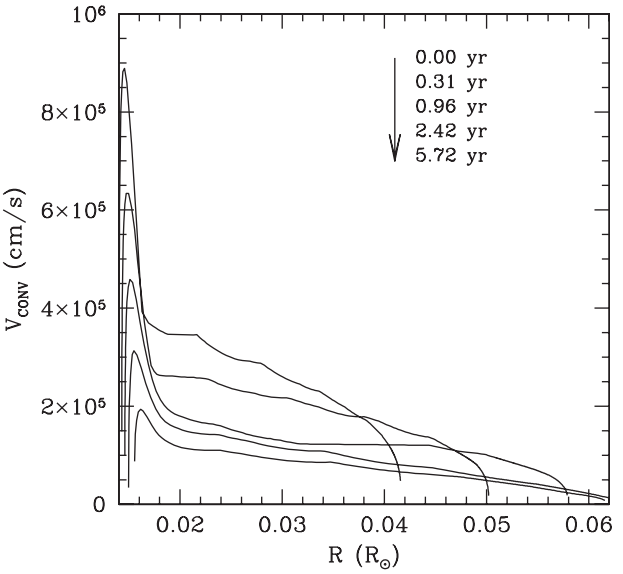

Figure 2 The calculated convective velocities as a function of the internal radius for 5 models ($t = 0$, 0.31, 0.96, 2.42, and 5.72 yr after the maximum of the TP) in a 3-$M_\odot$ star of solar composition. The convective turnover time is a few hours only. The scale on the abscissa starts at the bottom of the convective shell.

calculated convective velocities are plotted for five models ($t = 0$, 0.31, 0.96, 2.42, and 5.72 yr after the maximum of the TP) as a function of the internal radius to show how the convective shell expands after the pulse maximum.

The rather short convective turnover times of less than one hour that can be derived from Figure 2 are in any case, shorter than the time during which the temperature at the bottom of the convective pulse remains higher than 2.5×10^8 K. Hence, the crucial transport time from the hot synthesis zone to cooler layers is only of the order of minutes. This can have an impact on those potential *s*-process branchings, which are characterized by branch-point isotopes with strong thermal enhancements of their decay rates. Even if such half-lives are reduced to a few minutes at the bottom of the He shell flash, the signature of the branching can survive by the rapid mixing of processed material into the cooler outer layers of the convective zone.

2.3 Branching Analysis at A = *127/128*

The (n, γ) cross sections required for describing the time evolution of the ^{128}Xe and ^{130}Xe abundances during the He shell flashes have been accurately measured (Reifarth et al. 2002; Reifarth & Käppeler 2002). This information is crucial in view of the fact that only a comparably small fraction of the reaction flow is bypassing ^{128}Xe (Table 1). With the Xe cross sections compiled by Bao et al. (2000) for example, the ^{128}Xe/^{130}Xe ratio could only be calculated with an uncertainty of about 20%, whereas this uncertainty was reduced to ± 1.5% with the improved cross section data. Another source of uncertainty in the nuclear input is due to the theoretical β-decay rates listed in Table 1, which gives the β-decay branching ratio f_- at ^{128}I as a function of electron density n_e and temperature

Downloaded from https://www.cambridge.org/core. IP address: 3.89.132.163, on 17 Jan 2022 at 00:26:57, subject to the Cambridge Core terms of use, available at https://www.cambridge.org/core/terms. https://doi.org/10.1071/AS08052

(Takahashi & Yokoi 1987). Variation of these rates by a factor of two affects the branching ratio by less than 2%, because the decay of ^{128}I is dominated by the β^- mode.

In fact, the branching analysis indicates a more complex situation than one might expect from the trends of the branching factor in Table 1. During the low temperature phase between He shell flashes, the neutron density produced via the ^{13}C$(\alpha, n)^{16}$O reaction is less than 10^7 cm^{-3}. The branching at ^{127}Te is completely closed, resulting in a ^{128}Xe/^{130}Xe abundance ratio of 0.93 relative to the solar values at the end of the low temperature phase due to the effect of the ^{128}I branching. After the onset of convection at the beginning of the He shell flash the production factors of ^{128}Xe and ^{130}Xe differ by 8%, corresponding to the solar ratio, but are then modified during the flash. Since the (n, γ) cross sections of both isotopes are large enough for achieving local $\langle\sigma\rangle N_s$ equilibrium, one would expect that the production factor of ^{128}Xe quickly approaches that of ^{130}Xe. In this case, the final abundance ratio would clearly exceed the solar value.

In contrast, one finds that the branching still exists even during the high temperature phase of the He shell flash. There are essentially two effects, which concur to explain this behavior:

- During the peak of temperature and neutron density, the electron densities at the bottom of the convective He shell flash, i.e. in the *s*-process zone, are between 15×10^{26} cm^{-3} and 20×10^{26} cm^{-3}. Therefore, the branching at ^{128}I is never completely closed. Even at the peak temperatures of the He-shell flash, typically 3% of the flow are bypassing ^{128}Xe.
- Around the maximum of the neutron density, the branching at ^{127}Te is no longer negligible and leads to an additional decrease of the ^{128}Xe abundance.

In view of these effects the ^{127}Te branching can be fully understood only if the stellar reaction network is calculated with sufficiently small time steps so that the time scale of convective turnover is properly considered. If the neutron density is followed in time steps of 10^5 s up to freeze-out one finds an enhancement of the ^{127}Te branching of 30% compared to calculations performed on a time grid of 10^6 s. However, reducing the time steps to 3×10^4 s had no further effect on the abundance ratios.

If averaged over the AGB evolution, the stellar models yield a final abundance ratio of ^{128}Xe/^{130}Xe $= 0.466 \pm 0.015$, consistent with the smaller value measured in the solar system, 0.510 ± 0.005 if an 8% *p*-process contribution to the solar ^{128}Xe abundance is taken into account.

In summary, the abundance ratio of ^{128}Xe and ^{130}Xe in the solar system could be eventually reproduced by combining the effects of mass density, temperature, neutron density, and convective turnover in a consistent way. This success represents an impressive confirmation of the stellar *s*-process model related to thermally pulsing low mass AGB stars.

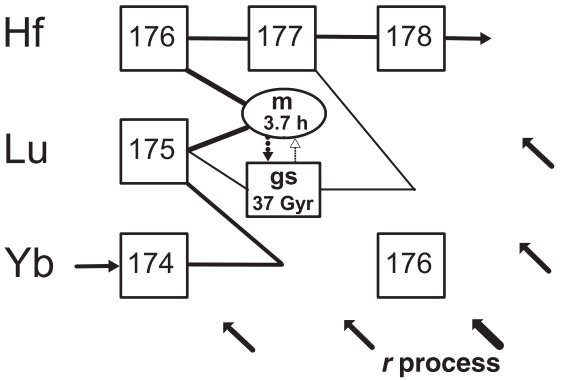

Figure 3 The *s*-process reaction flow in the Lu region. The strength of the lines indicates that neutron captures on ^{175}Lu leading to the isomeric state in ^{176}Lu are more probable than those to the ground state.

3 The ^{176}Lu/^{176}Hf Pair

The mass region of the rare earth elements (REE) represents an important test ground for *s*-process models because the relative REE abundances are known to better than ±2%, which implies that the branchings in this region are reliably defined by the respective *s*-only isotopes. Systematic analyses of these branchings contribute essentially to the quantitative picture of the main *s*-process component that has been achieved with stellar models for thermally pulsing low mass AGB stars (Gallino et al. 1998; Busso et al. 1999). Also the stellar (n, γ) cross sections (except for the lightest REE) are large enough that the assumption of reaction flow equilibrium is well justified with respect to the analysis of several prominent *s*-process branchings in this mass region. This means that the final abundances are essentially determined during the freeze-out phase at the decline of neutron density towards the end of the shell flash.

Among the REE branchings, ^{176}Lu is especially attractive for the intricate way in which nuclear physics can affect the actual *s*-process production yields. This is illustrated in Figure 3 showing that the reaction path in the vicinity of lutetium is determined not only by the stellar neutron-capture cross sections of ^{175,176}Lu and ^{176}Hf, but also by the thermal coupling of isomer and ground state in ^{176}Lu.

Due to its long half-life of 37.5 Gyr, ^{176}Lu was initially considered as a potential nuclear chronometer for the age of the *s* elements (Audouze, Fowler & Schramm 1972). This possibility is based on the fact that ^{176}Lu as well as its daughter ^{176}Hf are of pure *s*-process origin, since both are shielded against the *r*-process β-decay chains by their stable isobar ^{176}Yb. In a straightforward approach, the reaction flow in the branching at $A = 176$ and, therefore, the surviving *s* abundance of ^{176}Lu and of ^{176}Hf would be determined by the partial (n, γ) cross sections of ^{175}Lu feeding the ground and isomeric state of ^{176}Lu. Since transitions between the two states are highly forbidden by selection rules, both states could be considered as separate species in the description of the *s*-process

Downloaded from https://www.cambridge.org/core. IP address: 3.89.132.163, on 17 Jan 2022 at 00:26:57, subject to the Cambridge Core terms of use, available at https://www.cambridge.org/core/terms.
https://doi.org/10.1071/AS08052

branching at $A = 176$ (Figure 4). While the isomer decays quickly ($t_{1/2} = 3.7$ h) by β-transitions to ^{176}Hf, the effective *s*-process yield of ^{176}Lu appeared well defined by the partial cross section to ground state, thus providing an estimate of the age of the *s* elements by comparison with the actual solar system value.

However, Ward & Fowler (1980) noted that ground state and isomer of ^{176}Lu are most likely connected by nuclear excitations in the hot stellar-photon bath, since thermal photons at *s*-process temperatures are energetic enough to populate higher lying states, which can decay to the long-lived ground state and to the short-lived 123 keV isomer as well. In this way, the strict forbiddeness of direct transitions between both states is circumvented, dramatically reducing the effective half-life to a few hours. As a result, most of the reaction flow could have been directly diverted to ^{176}Hf, resulting in a ^{176}Lu abundance much smaller than observed in the solar system. That this temperature dependence had indeed affected the ^{176}Lu/^{176}Hf abundance ratio was confirmed soon thereafter by Beer et al. (1981, 1984), thus changing its interpretation from a potential chronometer into a sensitive *s*-process thermometer.

The temperature dependence was eventually quantified on the basis of a comprehensive investigation of the level structure of ^{176}Lu (Klay et al. 1991a,b; Doll et al. 1999). The lowest mediating state was identified at an excitation energy of 838.6 keV, which implies that thermally induced transitions become effective at temperatures above $T_8 = 1.5$–2 (where T_8 is the temperature in units of 10^8 K). Accordingly, ground state and isomer can be treated as separate species only at lower temperatures. In thermally pulsing low mass AGB stars this is the case between convective He shell flashes when the neutron production is provided by the ^{13}C$(\alpha, n)^{16}$O reaction in the so-called ^{13}C pocket. Under these conditions the abundance of ^{176}Lu is directly determined by the partial cross sections populating ground state and isomer.

During the He shell flashes, the higher temperatures at the bottom of the convective region lead to the activation of the ^{22}Ne$(\alpha, n)^{25}$Mg reaction. It is in this regime that the initial population of ground state and isomer starts to be changed by thermally induced transitions. This affects the ^{176}Lu$^{\rm g}$ in the long-lived ground state that is actually produced by neutron capture in the burning zone as well as in the Lu fraction circulating in the convective He shell flash. The latter part is exposed to the high bottom temperature only for rather short times and, therefore, less affected by the temperature dependence of the half life. Once produced, by far most of the long-lived ^{176}Lu$^{\rm g}$ survives in the cooler layers outside of the actual burning zone.

3.1 Nuclear-Physics Input

The stellar neutron-capture rates for describing the reaction flow in Figure 3 were determined by accurate time-of-flight (TOF) measurements of the total (n, γ) cross sections for ^{175}Lu and ^{176}Lu using a 4π BaF_2 array (Wisshak et al. 2006). The Maxwellian averaged cross sections (MACS) deduced from these data are five times more accurate than the values listed in the compilation of Bao et al. (2000). However, neutron captures on ^{175}Lu may feed either the ground state or the isomer in ^{176}Lu. Therefore, the total (n, γ) cross section had to be complemented by a measurement of at least one of the two partial cross sections $(\sigma_p^{\rm g}, \sigma_p^{\rm m})$. Since the corresponding reaction channels could not be distinguished in the TOF measurement (Wisshak et al. 2006), the activation technique was used to determine the partial cross section to the isomeric state in ^{176}Lu at thermal energies of $kT = 5.1$ and 25 keV.

Activation measurements of the partial (n, γ) cross section to the isomeric state in ^{176}Lu at or near a neutron energy of 25 keV were performed via the ^{7}Li$(p, n)^7$Be reaction (Beer & Käppeler 1980; Allen, Lowenthal & de Laeter 1981; Zhao & Käppeler 1991) and also using a filtered neutron beam from a nuclear reactor (Stecher-Rasmussen et al. 1988). In all experiments the induced activity after irradiation was detected via the 88 keV γ-transition in the decay of ^{176}Lu$^{\rm m}$. These data were recently complemented by an activation at $kT = 5$ keV, adapted to the lower temperature in the ^{13}C pocket Heil et al. (2008), where most of the neutron exposure is provided by the ^{13}C$(\alpha, n)^{16}$O source, which operates at $kT = 8$ keV.

The half-life of ^{176}Lu was shown to decrease drastically at the temperatures reached during He shell burning in thermally pulsing low mass AGB stars (Klay et al. 1991a; Doll et al. 1999). Contrary to the situation at low excitation energy, where transitions between ground state and isomer are strictly forbidden by selection rules, interactions with the hot stellar-photon bath lead to induced transitions to higher lying nuclear states, which can decay into the ground state and into the isomer as well (Figure 4).

Up to $T_8 = 2$ the mediating states can not be reached and the reaction path of Figure 3 is completely defined by the partial capture cross sections feeding ground state and isomer in ^{176}Lu. This situation prevails in the ^{13}C pocket between He shell flashes. Between $T_8 = 2.2$ and 3.0, ground state and isomer start to be increasingly coupled. At first, this coupling leads to an increasing population of the ground state, because of the smaller energy difference between isomer and mediating state. It is due to this effect that more ^{176}Lu is observed in nature than would be created in a 'cool' environment with $T_8 \leq 2$. In this regime, internal transitions, β decays, and neutron captures are equally important and have to be properly considered during He shell flashes, where the final abundance pattern of the *s*-process branchings are established by the marginal activation of the ^{22}Ne$(\alpha, n)^{25}$Mg neutron source reaction at thermal energies around $kT = 23$ keV.

3.2 Branching Factor

The branching factor $f_{\rm n}$ describing the split of the reaction flow at ^{176}Lu (Figure 3) can be expressed in terms of the neutron capture rate $\lambda_{\rm n} = \langle\sigma_{176}\rangle v_{\rm T} n_{\rm n}$ (where σ_{176} denotes the MACS of ^{176}Lu, $v_{\rm T}$ the mean thermal neutron velocity,

Downloaded from https://www.cambridge.org/core. IP address: 3.89.132.163, on 17 Jan 2022 at 00:26:57, subject to the Cambridge Core terms of use, available at https://www.cambridge.org/core/terms.
https://doi.org/10.1071/AS08052

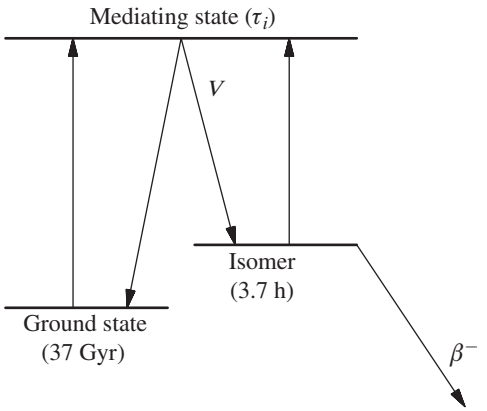

Figure 4 Schematic level scheme of ^{176}Lu illustrating the thermal coupling between the long-lived ground state and the short-lived isomer. While direct transitions between these states are strictly forbidden by selection rules, thermal excitations in the hot stellar-photon bath populate a higher lying state with intermediate quantum numbers that can decay both ways. At first this link depopulates the isomer towards the ground state because it is more easily reached from the isomer. However, at sufficiently high temperatures, induced transitions from the ground state to the mediating state can also feed the isomer, resulting in the destruction of ^{176}Lu via β decay of the short-lived isomer. The efficiency of this mechanism is determined by the lifetime τ_i of the mediating state and by the branching ratio V for decays towards the isomer.

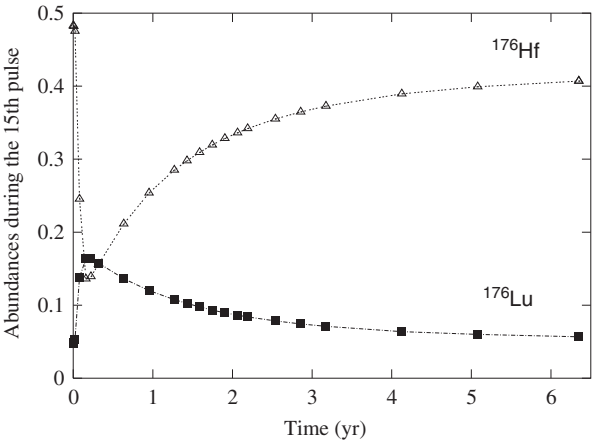

Figure 5 Evolution of the ^{176}Lu (squares) and ^{176}Hf (circles) abundances during the 15th He shell flash in an AGB star with 1.5 $M_\odot$. The time scale starts when the temperature at the bottom of the convective shell reaches $T_8 = 2.5$, i.e. at the onset of the ^{22}Ne$(\alpha, n)^{25}$Mg reaction. The values are given as number fractions normalized to that of ^{150}Sm at the end of the He shell flash.

and n_n the neutron density) and of the temperature and neutron density dependent β-decay rate of ^{176}Lu. Because of the thermal effects on the lifetime of ^{176}Lu sketched above, $f_n = \lambda_n/(\lambda_n + \lambda_\beta)$ becomes a complex function of temperature and neutron density (Klay et al. 1991a; Doll et al. 1999).

The bottom temperature in the He flashes reaches a maximum at the maximum expansion of the convection zone and then declines rapidly as the convective thermal instability shrinks. According to current AGB models of low mass stars, the neutron burst released by the ^{22}Ne neutron source lasts for about six years, as long as $T_8 \geq 2.5$, while the convective instability lasts for a much longer period of about 150 years. The maximum temperature in the He flash increases slightly with pulse number, reaching $T_8 \approx 3$ in the more advanced pulses (Straniero et al. 2003).

Although the second neutron burst during the He shell flashes contributes only a few percent to the total neutron exposure, the final composition of the Lu/Hf branching is, in fact, established during the freeze-out phase at the end of the thermal pulse. It is only during the high-temperature phase that the thermal coupling between ground state and isomer takes place. In this context, it is also important to remember that the (n, γ) cross sections in the Lu/Hf region are large enough that typical neutron capture times are significantly shorter than the duration of the neutron exposure during the He shell flash.

Previous *s*-process calculations for thermally pulsing low mass AGB stars (Gallino et al. 1988, 1998), which were performed by post-processing using full stellar evolutionary models obtained with the FRANEC code (Chieffi & Straniero 1989; Straniero et al. 1995; Straniero et al. 2003; Straniero, Gallino & Cristallo 2006) were successful in describing the solar main *s*-process component fairly well (Gallino et al. 1998; Arlandini et al. 1999). For the treatment of the branching at ^{176}Lu, however, this approach had to be refined by subdividing the convective region of the He shell flashes into 30 meshes in order to follow the neutron density profile in sufficient detail and to take the strong temperature dependence of the branching factor f_n properly into account. The production and decay of ^{176}Lu was calculated in each mesh to obtain an accurate description of the final ^{176}Lu/^{176}Hf ratio in the He shell flash.

After each time step of less than one hour, which corresponds to the typical turnover time for convection in the He shell flash (Reifarth et al. 2004), the abundances from all zones were averaged in order to account for the fast convective mixing. This treatment is well justified because there is no efficient coupling between ground state and isomer at temperatures below $T_8 \leq 2.5$, which holds for all meshes except the first few from the bottom. Interestingly, this is the temperature when neutron production via the ^{22}Ne$(\alpha, n)^{25}$Mg reaction diminishes.

During the main neutron exposure provided by the ^{13}C$(\alpha, n)^{16}$O reaction thermal effects are negligible for the production of ^{176}Lu because the temperatures in the ^{13}C pocket of $T_8 \approx 1$ are not sufficient to reach the mediating state at 838.6 keV. Accordingly, the ^{176}Lu/^{176}Hf ratio is simply determined by the partial (n, γ) cross section to the ground state, which would always produce too much ^{176}Hf and too little ^{176}Lu^g. This situation is illustrated in Figure 5 showing the relative production factors of ^{176}Lu and ^{176}Hf during the 15th He shell flash of the AGB model with initial mass 1.5 $M_\odot$ and half-solar metallicity, which is representative of the overall relative abundance distribution ejected during the AGB phase. The *s*-process abundances are given as number fractions $Y_i = X_i/A_i$ (X

Downloaded from https://www.cambridge.org/core. IP address: 3.89.132.163, on 17 Jan 2022 at 00:26:57, subject to the Cambridge Core terms of use, available at https://www.cambridge.org/core/terms.
https://doi.org/10.1071/AS08052

being the respective mass fractions), normalized to that of ^{150}Sm at the end of the He shell flash. This isotope was chosen as a reference because it is the best known case of an unbranched *s*-only isotope among the REE.

After the *s*-process nuclides synthesized in the ^{13}C pocket are engulfed by the convective He shell, one finds the ratio shown at $t = 0$ in Figure 5, which marks the onset of *s*-process nucleosynthesis in the He shell flash. In this phase temperatures are high enough to populate the mediating state at 838 keV, leading to a strong increase in the production of the long-lived ground state of ^{176}Lu^{g}. As shown in Figure 5, ^{176}Hf is almost completely destroyed at the beginning of the flash, when neutron density and temperature are highest and ^{176}Hf is efficiently bypassed by the reaction flow. Correspondingly, the ^{176}Lu abundance reaches a pronounced maximum. As temperature and neutron density decline with time, the branching towards ^{176}Hf is more and more restored, but the final abundance at the end of the He shell flash remains significantly lower than at the beginning. Because the thermal coupling between ground state and isomer depends so critically on temperature, the full *s*-process network was followed in each of the 30 meshes of the convective zone.

Plausible solutions of the Lu/Hf puzzle are characterized by equal overproduction factors for ^{176}Lu and ^{176}Hf, at least within the experimental uncertainties of the nuclear input data. The decay of long-lived ^{176}Lu ground state in the interstellar medium prior to the formation of the solar system reduces the calculated overproduction factor of ^{176}Lu by about 10%, leaving the more abundant ^{176}Hf essentially unchanged. In the light of these considerations, overproduction factors between 1.00 and 1.10 are acceptable for ^{176}Lu and between 0.95 and 1.05 for ^{176}Hf.

In the course of these investigations it turned out that the observed ^{176}Lu/^{176}Hf ratio could only be reproduced if the thermal coupling of ground state and isomer in ^{176}Lu in combination with the neutron density was followed within the gradients of time, mass, and temperature by the refined zoning of the convective He shell flash. Only in this way overproduction factors could be obtained, which were compatible with the limits defined by the nuclear physics uncertainties and by the ^{176}Lu decay. In contrast to a previous study (Arlandini et al. 1999), the meanwhile improved cross section information together with the multi-zone approach for the He shell flash appears to settle the ^{176}Lu puzzle. While the ^{176}Hf abundance was before overproduced by 10–20%, the present calculations yield final ^{176}Lu^{g} and ^{176}Hf abundances (relative to solar system values) of 1.04 and 0.96. These results do not yet consider the decay of the produced ^{176}Lu^{g}, a correction that brings the two numbers even into closer agreement.

Recently, additional information from Coulomb excitation measurements (Vanhorenbeek et al. 2000) and photoactivation studies (Kneissl 2005) have triggered renewed interest in the Lu/Hf problem (Mohr 2008) and seem to provide further constraints for the convection at the bottom of the He shell flash.

4 Conclusions

The elemental and isotopic abundances found in nature carry the signatures of their nucleosynthetic origin as well as of the related time scales. The branchings at ^{128}I and ^{176}Lu discussed in Sections 2 and 3 are characterized by the rather short time scale of convection in He shell flashes of low mass AGB stars. Examples dealing with much longer time scales are discussed by R. Reifarth and A. Mengoni in their contributions to this volume.

To decipher the information contained in abundance patterns can be an intricate and complex process, which requires

- accurate nuclear physics data, in particular the rates for production and transmutation by nuclear reactions, but often also nuclear structure properties for describing the impact of temperature, and
- sufficiently detailed astrophysical prescriptions for a realistic or at least plausible modeling of the relevant phenomena. It is this duality that we had the pleasure to pursue in the Torino–FZK liaison for more than two decades, and which, in return, was found to provide surprising constraints for the physics of stellar evolution.

References

Allen, B. J., Lowenthal, G. C. & de Laeter, J. R., 1981, JPhGS, 7, 1271
Arlandini, C., Käppeler, F., Wisshak, K., Gallino, R., Lugaro, M., Busso, M. & Straniero, O., 1999, ApJ, 525, 886
Arnould, M., 1973, A&A, 22, 311
Arnould, M. & Goriely, S., 2003, PhR, 384, 1
Arnould, M., Takahashi, K. & Yokoi, K., 1984, A&A, 137, 51
Audouze, J., Fowler, W. A. & Schramm, D. N., 1972, NPhS, 238, 8
Bao, Z. Y., Beer, H., Käppeler, F., Voss, F., Wisshak, K. & Rauscher, T., 2000, ADNDT, 76, 70
Beer, H. & Käppeler, F., 1980, PhRvC, 21, 534
Beer, H. & Walter, G., 1984, Ap&SS, 100, 243
Beer, H. & Penzhorn, R.-D., 1987, A&A, 174, 323
Beer, H., Käppeler, F., Wisshak, K. & Ward, R. A., 1981, ApJS, 46, 295
Beer, H., Walter, G., Macklin, R. L. & Patchett, P. J., 1984, PhRvC, 30, 464
Best, J., Stoll, H., Arlandini, C., Jaag, S., Käppeler, F., Wisshak, K., Mengoni, A., Reffo, G. & Rauscher, T., 2001, PhRvC, 64, 15801
Busso, M., Lambert, D. L., Beglio, L., Gallino, R., Raiteri, C. M. & Smith, V. V., 1995, ApJ, 446, 775
Busso, M., Gallino, R. & Wasserburg, G. J., 1999, ARA&A, 37, 239
Chieffi, A. & Straniero, O., 1989, ApJS, 71, 47
Cowan, J. J., Pfeiffer, B., Kratz, K.-L., Thielemann, F.-K., Sneden, C., Burles, S., Tytler, D. & Beers, T. C., 1999, ApJ, 521, 194
Doll, C., Börner, H., Jaag, S. & Käppeler, F., 1999, PhRvC, 59, 492
Gallino, R., Busso, M., Picchio, G., Raiteri, C. M. & Renzini, A., 1988, ApJ, 334, L45
Gallino, R., Arlandini, C., Busso, M., Lugaro, M., Travaglio, C., Straniero, O., Chieffi, A. & Limongi, M., 1998, ApJ, 497, 388
Heil, M., Winckler, N., Dababneh, S., Käppeler, F., Wisshak, K., Bisterzo, S., Gallino, R., Davis, A. M. & Rauscher, T., 2008, ApJ, 673, 434
Klay, N., Käppeler, F., Beer, H. & Schatz, G., 1991, PhRvC, 44, 2839
Klay, N. et al., 1991, PhRvC, 44, 2801
Kneissl, U., 2005, Bulg. Nucl. Sci. Trans., 10, 55

Downloaded from https://www.cambridge.org/core. IP address: 3.89.132.163, on 17 Jan 2022 at 00:26:57, subject to the Cambridge Core terms of use, available at https://www.cambridge.org/core/terms. https://doi.org/10.1071/AS08052

Mathews, G. J., Takahashi, K., Ward, R. A. & Howard, W. M., 1986, ApJ, 302, 410
Mohr, P., 2008, PoS, NIC X, 081
Mosconi, M. et al., 2007, PrPNP, 59, 165
Pagel, B. E. J., 1990, in Astrophysical Ages and Dating Methods, Eds. Vangioni-Flam, E., Cassé, M., Audouze, J. & Tran Thanh Van, J. (Gif sur Yvette: Editions Frontières), 493
Pepin, R. O., Becker, R. H. & Rider, P. E., 1995, GeCoA, 59, 4997
Reifarth, R. & Käppeler, F., 2002, PhRvC, 66, 054605
Reifarth, R. et al., 2002, PhRvC, 66, 064603
Reifarth, R., Käppeler, F., Voss, F., Wisshak, K., Gallino, R., Pignatari, M. & Straniero, O., 2004, ApJ, 614, 363
Schatz, G., 1983, A&A, 122, 327
Smith, V. V. & Lambert, D. L., 1988, ApJ, 333, 219
Stecher-Rasmussen, F., Abrahams, K., Kopecky, J., Lindner, J. & Polak, P., 1988, in Inst. Phys. Conf. Ser. 88, Capture Gamma-Ray Spectroscopy 1987, Eds. Abrahams, K. & Van Assche, P. (Bristol: Institute of Physics), 754
Straniero, O., Gallino, R., Busso, M., Chieffi, A., Raiteri, C. M., Limongi, M. & Salaris, M., 1995, ApJ, 440, L85
Straniero, O., Chieffi, A., Limongi, M., Busso, M., Gallino, R. & Arlandini, C., 1997, ApJ, 478, 332
Straniero, O., Domínguez, I., Cristallo, R. & Gallino, R., 2003, PASA, 20, 389
Straniero, O., Gallino, R. & Cristallo, S., 2006, NPhA, 777, 311
Takahashi, K. & Yokoi, K., 1987, ADNDT, 36, 375
Vanhorenbeek, J., Lagrange, J. M., Pautrat, M., Dionisio, J. S. & Vieu, Ch., 2000, PhRvC, 62, 015801
Ward, R. A. & Fowler, W. A., 1980, ApJ, 238, 266
Wisshak, K. et al., 2001, PhRvL, 87, 251102
Wisshak, K., Voss, F., Käppeler, F. & Kazakov, L., 2006, PhRvC, 73, 015807
Yokoi, K., Takahashi, K. & Arnould, M., 1983, A&A, 117, 65
Yokoi, K., Takahashi, K. & Arnould, M., 1985, A&A, 145, 339
Zhao, W. R. & Käppeler, F., 1991, PhRvC, 44, 506

Downloaded from https://www.cambridge.org/core. IP address: 3.89.132.163, on 17 Jan 2022 at 00:26:57, subject to the Cambridge Core terms of use, available at https://www.cambridge.org/core/terms. https://doi.org/10.1071/AS08052